






A gibberellin methyltransferase modulates the timing of floral transition at the *Arabidopsis* shoot meristem

Joanne E. Lee^a,  Daniela Goretti^{a,†},  Manuela Neumann^b,  Markus Schmid^{a,b,c,*}  and Yuan You^{b,d,*} 

^aUmeå Plant Science Centre, Department of Plant Physiology, Umeå University, Umeå SE-901 87, Sweden

^bDepartment of Molecular Biology, Max Planck Institute for Developmental Biology, Tübingen 72076, Germany

^cBeijing Advanced Innovation Centre for Tree Breeding by Molecular Design, Beijing Forestry University, Beijing 100083, People's Republic of China

^dCenter for Plant Molecular Biology (ZMBP), Department of General Genetics, University Tübingen, Tübingen 72076, Germany

Correspondence

Corresponding authors,

*e-mails: markus.schmid@umu.se; yuan.you@zmbp.uni-tuebingen.de

Received 15 March 2020;

revised 26 May 2020

doi:10.1111/ppl.13146

The transition from vegetative to reproductive growth is a key event in the plant life cycle. Plants therefore use a variety of environmental and endogenous signals to determine the optimal time for flowering to ensure reproductive success. These signals are integrated at the shoot apical meristem (SAM), which subsequently undergoes a shift in identity and begins producing flowers rather than leaves, while still maintaining pluripotency and meristematic function. Gibberellic acid (GA), an important hormone associated with cell growth and differentiation, has been shown to promote flowering in many plant species including *Arabidopsis thaliana*, but the details of how spatial and temporal regulation of GAs in the SAM contribute to floral transition are poorly understood. In this study, we show that the gene *GIBBERELLIC ACID METHYLTRANSFERASE 2* (*GAMT2*), which encodes a GA-inactivating enzyme, is significantly upregulated at the SAM during floral transition and contributes to the regulation of flowering time. Loss of *GAMT2* function leads to early flowering, whereas transgenic misexpression of *GAMT2* in specific regions around the SAM delays flowering. We also found that *GAMT2* expression is independent of the key floral regulator *LEAFY* but is strongly increased by the application of exogenous GA. Our results indicate that *GAMT2* is a repressor of flowering that may act as a buffer of GA levels at the SAM to help prevent premature flowering.

Introduction

Floral transition, the shift from vegetative to reproductive growth, has major impacts on species' survival and

reproductive success, particularly in annual plants such as *Arabidopsis thaliana* and many crop species (Wilczek et al. 2009). As such, plants utilise a variety of

Abbreviations – AD, activation domain; AP1, APETALA 1; ChIP-chip, chromatin immunoprecipitation coupled to microarray; CL, cauline leaf; CLN, cauline leaf number; CO, CONSTANS; CZ, central zone; ELA1, EUI-LIKE P450 A1; EUI1, ELONGATED UPPER-MOST INTERNODE1; FT, FLOWERING LOCUS T; GA, gibberellic acid; GA2Ox2, GIBBERELLIN 20 OXIDASE 2; GAMT1, GIBBERELLIC ACID METHYLTRANSFERASE 1; GAMT2, GIBBERELLIC ACID METHYLTRANSFERASE 2; IM, inflorescence meristem; IM-I, inflorescence meristem phase I; IM-II, inflorescence meristem phase II; KNOX, KNOTTED1-LIKE HOMEOBOX; L1, layer 1; L2, layer 2; LD, long day; LFY, LEAFY; P0, floral primordia 0; P1, floral primordia 1; PZ, peripheral zone; qPCR, quantitative PCR; RLN, rosette leaf number; RT-PCR, reverse transcription-PCR; RZ, rib zone; SAM, shoot apical meristem; SD, short day; SOC1, SUPPRESSOR OF OVEREXPRESSION OF CONSTANS 1; TSF, TWIN SISTER OF FT; TUB2, TUBULIN BETA CHAIN 2; UBC21, UBIQUITIN-CONJUGATING ENZYME 21; VM, vegetative meristem; ZT, Zeitgeber time.

[†]Present address: Department of Forest Genetics and Plant Physiology, Umeå Plant Science Centre, Swedish University of Agricultural Sciences, Umeå SE-901 87, Sweden

environmental and endogenous signals, which may be perceived in leaves and/or other parts of the plant, to ensure that flowering occurs at the optimal time (Wilczek et al. 2009). In *Arabidopsis*, these floral inductive signals are processed via a complex regulatory network involving numerous interacting pathways (Srikanth and Schmid 2011), which are ultimately integrated at the shoot apical meristem (SAM), where they activate expression of flowering time genes such as *SUPPRESSOR OF OVEREXPRESSION OF CONSTANS 1* (*SOC1*) and the floral meristem identity genes *APETALA 1* (*AP1*) and *LEAFY* (*LFY*) (Immink et al. 2012). Transcriptional reprogramming of cells in the SAM results in a shift in identity from a rosette leaf-producing vegetative meristem (VM) to a reproductive inflorescence meristem (IM), which produces cauline leaves during inflorescence meristem phase I (IM-I) and floral primordia during inflorescence meristem phase II (IM-II) (Ratcliffe et al. 1999, Yamaguchi et al. 2014).

Gibberellic acid (GA) is a plant hormone that plays diverse roles in plant growth and development (Olszewski et al. 2002). Bioactive GAs (GA_1 , GA_3 , GA_4 and GA_7) are generally concentrated at growth centres such as developing lateral organ primordia, where they promote cell growth and differentiation (Olszewski et al. 2002), and they also act as floral inductive signals via the GA-signalling pathway (Fornara et al. 2010, Srikanth and Schmid 2011, Bao et al. 2020). In long-day (LD) growth conditions, GAs act in parallel with the photoperiod-regulated transcription factor *CONSTANS* (*CO*) to induce flowering by promoting expression of the key floral regulators *FLOWERING LOCUS T* (*FT*) and *TWIN SISTER OF FT* (*TSF*) in leaves (Srikanth and Schmid 2011). *FT* and *TSF* are subsequently transported to the SAM, where they interact with and modulate the DNA-binding and transcriptional activity of the bZIP transcription factor *FD* to promote flowering (Fornara et al. 2010, Srikanth and Schmid 2011). In short-day (SD) growth conditions, GAs are required to promote expression at the *LFY* promoter (Blazquez et al. 1997, Blazquez and Weigel 2000), such that the GA-deficient *ga1-3* mutant is unable to flower in SDs due to almost complete loss of *LFY* and *SOC1* expression (Blazquez et al. 1998, Moon et al. 2003).

Although the importance of GAs in flowering is well-established, the precise roles of bioactive GAs in SAM development and floral transition are complex and have not been characterised in great detail (Hay and Tsiantis 2010, Yamaguchi et al. 2014). This is largely due to the structure of the SAM, which is small in size but contains a number of clearly defined functional zones with different cell types: a central zone of undifferentiated, slowly dividing stem cells is surrounded by a peripheral

zone of rapidly proliferating cells that fuel lateral organ formation, and supported by the rib zone underneath, from which cells that form the stem tissues are derived (Weigel and Jurgens 2002). At the edges of the SAM, there is also a boundary region of restricted growth, which physically separates the SAM from adjacent lateral organs and has a number of other specialised functions (Scofield et al. 2018). It is technically challenging to either separate these tissues for chemical analysis or directly visualise GA distribution within the SAM, so the distribution of bioactive GAs has typically been inferred from the expression patterns of genes involved in GA biosynthesis, inactivation and signalling (Olszewski et al. 2002). For example, the gene encoding GA 20-oxidase, a rate-limiting enzyme that catalyses one of the final steps in the biosynthesis of bioactive GAs, is expressed in regions around the shoot apex but is excluded from the VM by the activity of *KNOTTED1-LIKE HOMEODOMAIN* (*KNOX*) transcription factors (Sakamoto et al. 2001, Hay et al. 2002). This indicates that the levels of bioactive GAs are kept low in the SAM, which is thought to be important for preventing cell differentiation and maintaining pluripotency (Hay and Tsiantis 2010). *KNOX* proteins also act to promote the expression of genes encoding GA-inactivating enzymes at the base of the VM and developing leaf primordia, which is suggested to set a boundary limiting diffusion of GA into the SAM (Jasinski et al. 2005, Bolduc and Hake 2009). During the transition to flowering, expression of *GIBBERELLIN 20 OXIDASE 2* (*GA20ox2*) is strongly induced in the rib zone and is thought to drive a rapid increase in GA levels in the SAM, thereby promoting floral transition (Andres et al. 2014). However, the subsequent shift from cauline leaf to flower formation requires a decrease in GA levels, which is mediated by the activity of the GA-inactivating enzyme *EUI-LIKE P450 A1* (*ELA1*) in floral primordia during the IM-II stage of development (Yamaguchi et al. 2014). *ELA1* expression is induced by *LFY* and *AP1*, and loss of *ELA1* function specifically affects the IM-I to IM-II transition, resulting in increased cauline leaf number and delayed flower formation. In *Arabidopsis*, there also exists another class of GA-inactivating enzymes, the *SABATH* family methyltransferases *GIBBERELIC ACID METHYLTRANSFERASE 1* (*GAMT1*) and *GIBBERELIC ACID METHYLTRANSFERASE 2* (*GAMT2*). These enzymes methylate a range of bioactive and non-bioactive GAs, which inactivates them and has been suggested to initiate the process of GA degradation (Varbanova et al. 2007, Xing et al. 2007). Both genes are expressed predominantly in siliques and have roles in seed development and germination (Varbanova et al. 2007, Xing et al. 2007), but no role in floral transition has previously been reported.

In this study, we show that *GAMT2* is strongly induced in peripheral and boundary regions of the SAM in response to inductive photoperiod. Loss of *GAMT2* function resulted in an early flowering phenotype, whereas misexpression of *GAMT2* at the shoot apex had the opposite effect, indicating that *GAMT2* is a floral repressor. Furthermore, mild floral patterning defects such as altered numbers of stamens were often observed in the *gamt2* mutants, suggesting that *GAMT2* may also play a role in floral patterning. Contrary to what was suggested by a previous study (Winter et al. 2011), we found no evidence that *GAMT2* expression is regulated by *LFY*, nor did *LFY* expression appear to be influenced by *GAMT2*, but *GAMT2* expression was strongly induced by the application of exogenous GA to the shoot apex. Together, these results suggest that *GAMT2* may act as part of a negative feedback loop that buffers GA levels to modulate the speed and timing of floral transition.

Materials and methods

Plant materials and growth

The *Arabidopsis thaliana* ecotype Columbia-0 (Col-0) was used as a wild-type control throughout this study. Seeds of *gamt2-1* (SALK_143728) and *gamt2-3* (SALK_043182) mutants were obtained from the Nottingham Arabidopsis Stock Centre. Homozygous *gamt2-1* and *gamt2-3* plants were identified by genotyping using primers designed by the online T-DNA Primer Design Tool (<http://signal.salk.edu/tdnaprimers.2.html>; Supporting Information Table S1). Seeds of *lfy-12* and *ap1-15* mutants were from lab stock of Professor Detlef Weigel (Max Planck Institute for Developmental Biology, Germany), and homozygous plants were identified as described previously (Blazquez et al. 1997, Gocal et al. 2001, Ng and Yanofsky 2001).

Seeds were stratified in 0.1% agar at 4°C for 3 days in the dark prior to sowing, to synchronise germination. For genotyping and phenotyping experiments, plants were typically grown in growth chambers on soil at constant 23 or 22°C during light periods and 18°C during dark periods, with 65% relative humidity. The growth chambers used a mixture of Cool White and Gro-Lux Wide Spectrum fluorescent lights, with a fluence rate of 125 to 175 $\mu\text{mol m}^{-2} \text{s}^{-1}$. LDs were 16 h light/8 h dark and SDs were 8 h light/16 h dark. For floral induction experiments, plants were grown on soil in SDs for 3 weeks before shifting to LDs (You et al. 2017).

Reverse transcription-PCR (RT-PCR)

Siliques were harvested from mature Col-0, *gamt2-1* and *gamt2-3* plants, and RNA was extracted using the RNeasy

Micro Kit (Qiagen). About 500 ng of total RNA was treated with DNase I (0.05 U per μl ; Thermo Fisher Scientific) for 30 min at 37°C to remove any contaminating genomic DNA, then used as the template for cDNA synthesis using the RevertAid First Strand cDNA Synthesis Kit (Thermo Scientific) with oligo dT primers. PCR amplification was performed using 0.5 μl of cDNA template with Taq polymerase for 30 cycles. Primer sequences are listed in Table S1.

Quantitative PCR (qPCR)

Shoot apex regions (approx. 2 mm³) were manually harvested from Col-0, *lfy-12*, *ap1-15*, *gamt2-1* and *gamt2-3* plants grown in SDs and/or LDs, as indicated in the text. Samples were typically collected at Zeitgeber time (ZT) 6–7. For the exogenous GA treatment, 3-week-old SD-grown Col-0 plants were treated with 5 μl of either 50 μM GA₃ with 0.01% Tween-20 or a mock solution of 0.01% Tween-20. The treatments were applied directly to the shoot apex at ZT 6, and shoot apices were manually harvested 20 h post-treatment. RNA extraction and cDNA synthesis were performed as described in the section Reverse transcription-PCR above. The cDNA was used as template in qPCR reactions using gene-specific primers (Table S1) with LightCycler 480 SYBR Green I Master Mix (Roche Life Science) in a Bio-Rad CFX96 machine. The house-keeping genes *UBIQUITIN-CONJUGATING ENZYME 21* (*UBC21*) or *TUBULIN BETA CHAIN 2* (*TUB2*) were used as controls. qPCR analysis was performed using three biological replicates of each treatment/genotype, with three technical replications per sample. Statistical analyses were performed using Student's *t*-test.

Plasmid constructs and plant transformation for *GAMT2* reporter and misexpression

For generating the *pGAMT2:VENUS-GAMT2:tGAMT2* reporter constructs and the *GAMT2* misexpression constructs *pAt3g59270:GAMT2:tAt3g59270*, *pAt3g59270:VENUS-GAMT2:tAt3g59270*, *pLAS:VENUS-GAMT2:tLAS* and *pKNAT1:VENUS-GAMT2:tRBCS*, *GAMT2* or N-terminal VENUS-tagged *GAMT2* coding sequence was cloned between gene-specific promoters and terminators by GreenGate cloning (Lampropoulos et al. 2013). The associated primer sequences used for the GreenGate plasmid modules generated in this study are listed in Table S1, and GreenGate entry plasmids used for the assemblies are summarised in Table S2. Phusion High-Fidelity DNA polymerase (Thermo Fisher Scientific) was used for PCR reactions. All constructs were verified by Sanger sequencing after cloning. The plasmid constructs were transformed into Col-0 plants using *Agrobacterium*

tumefaciens strain GV3101 (pSoup) by floral dip (Clough and Bent 1998). Transgenic plants were selected by spraying germinating seedlings with 0.1% (v/v) Basta.

Microscopy

Fluorescence of the VENUS-GAMT2 fusion protein in the transgenic lines was examined in the shoot apices of 16-day-old plants using a Zeiss LSM 780 confocal microscope with laser excitation at 514 nm. The images of wild-type Col-0 and *gamt2* mutant flowers were taken using a Leica MZ9.5 stereomicroscope. A ZEISS Axioplan 2 imaging system was used for imaging the in situ histological sections and the *pLAS:VENUS-GAMT2:tLAS* epifluorescence microscopy.

Probe synthesis and RNA in situ hybridisation

For the *GAMT2* probe, a 252 bp fragment of *GAMT2* was amplified from cDNA prepared from the shoot apices of Col-0 plants grown in SDs for 3 weeks and then shifted to LDs for 3 days (see section Quantitative PCR above), and cloned into the pGEM®-T vector by standard TA cloning (Promega). This fragment was subsequently reamplified using T7 and SP6 primers (Table S1), and used as a template for synthesising a digoxigenin-labelled anti-sense RNA probe to *GAMT2* mRNA using the DIG RNA labeling kit with T7 RNA polymerase (Roche). Similarly, a digoxigenin-labelled anti-sense RNA probe to *LFY* mRNA was prepared from plasmid pAM190 (a kind gift from Professor Alexis Maizel, University of Heidelberg), which contains the *LFY* coding region flanked by *EcoRI* (5') and *BamHI* (3') restriction sites in the pGEM®-T Easy vector (Promega).

For RNA in situ hybridisation, shoot apices of Col-0, *lfy-12* and *gamt2-3* plants were collected manually and immediately fixed in formaldehyde/acetic acid/ethanol (3.7/5/50%). Tissue was dehydrated through an ethanol series, stained with eosin, and infiltrated with molten Histowax. Embedded samples were then sectioned to 8 µm thickness and RNA in situ hybridisation was performed as described previously (Wang et al. 2009). The signal was developed by a colour reaction using NBT-BCIP solution (Roche).

Yeast one-hybrid constructs and assays

For the bait constructs, two *GAMT2* promoter fragments containing the putative LFY binding sites pGAMT2 site 1 & 2 (448 bp) and pGAMT2 site 3 (726 bp) were amplified by PCR, using the 3.9 kb *GAMT2* promoter from the *pGAMT2:VENUS-GAMT2:tGAMT2* reporter construct as a template, and cloned into pMW#3 (Deplancke et al. 2006) upstream of the *lacZ* reporter using *HindIII*. A 193 bp fragment of the *AP1* promoter containing the

primary LFY binding motif was amplified directly from genomic DNA and cloned into pMW#3 using the *HindIII* and *SalI* restriction sites. The prey construct was made by cloning the *LFY* coding sequence from the plasmid pAM190 into pGAD-T7 (Clontech), downstream of the GAL4 activation domain (AD) coding sequence, using the *EcoRI* site. Phusion High-Fidelity DNA polymerase (Thermo Fisher Scientific) was used for PCR reactions. The primers used are listed in Table S1 and all constructs were verified by Sanger sequencing.

Transformation of constructs into yeast and β-Gal colorimetric assays were performed as described previously (Deplancke et al. 2006). Bait constructs were linearized with *NcoI* and transformed into yeast strain YM4271. Integration was verified by PCR, and colonies were checked for reporter gene self-activation before being transformed with either the AD-LFY prey construct or empty pGAD-T7. Three independent colonies were selected for each bait-prey combination and tested for β-galactosidase activity.

Results

GAMT2 is expressed in the SAM and floral primordia during floral transition

In previous microarray experiments, we found that the gene *GAMT2* was strongly upregulated in the shoot apex during photoperiod-induced floral transition, suggesting a potential role in the regulation of flowering time (Fig. S1) (Schmid et al. 2005). To examine the expression of *GAMT2* during floral transition, we triggered synchronous flowering by shifting 21-day-old SD-grown Col-0 plants to LD conditions. We have previously shown that this treatment induces floral commitment within 2 to 3 days of growth in LDs (You et al. 2017, 2019). In agreement with our previous findings, qPCR analysis showed that *GAMT2* expression was low in the vegetative shoot apex prior to the shift but increased significantly on the second and third days after the shift to LDs (Fig. 1A).

To examine the expression pattern of *GAMT2*, we generated two different *pGAMT2:VENUS-GAMT2:tGAMT2* reporter lines using 3.9 and 6.5 kb *GAMT2* promoter fragments, in combination with an 0.8 kb *GAMT2* terminator fragment. However, we were unable to observe VENUS fluorescence at the SAM of transgenic plants, suggesting that other regulatory signals (e.g. further upstream of the 6.5 kb promoter or downstream of the 0.8 kb terminator) are required for *GAMT2* expression at the SAM. We therefore examined the spatiotemporal dynamics of *GAMT2* expression using the alternative approach of RNA in situ hybridisation. In vegetative SD-grown plants and in plants exposed to one LD, *GAMT2* transcripts were observed in the tips of leaf primordia but could

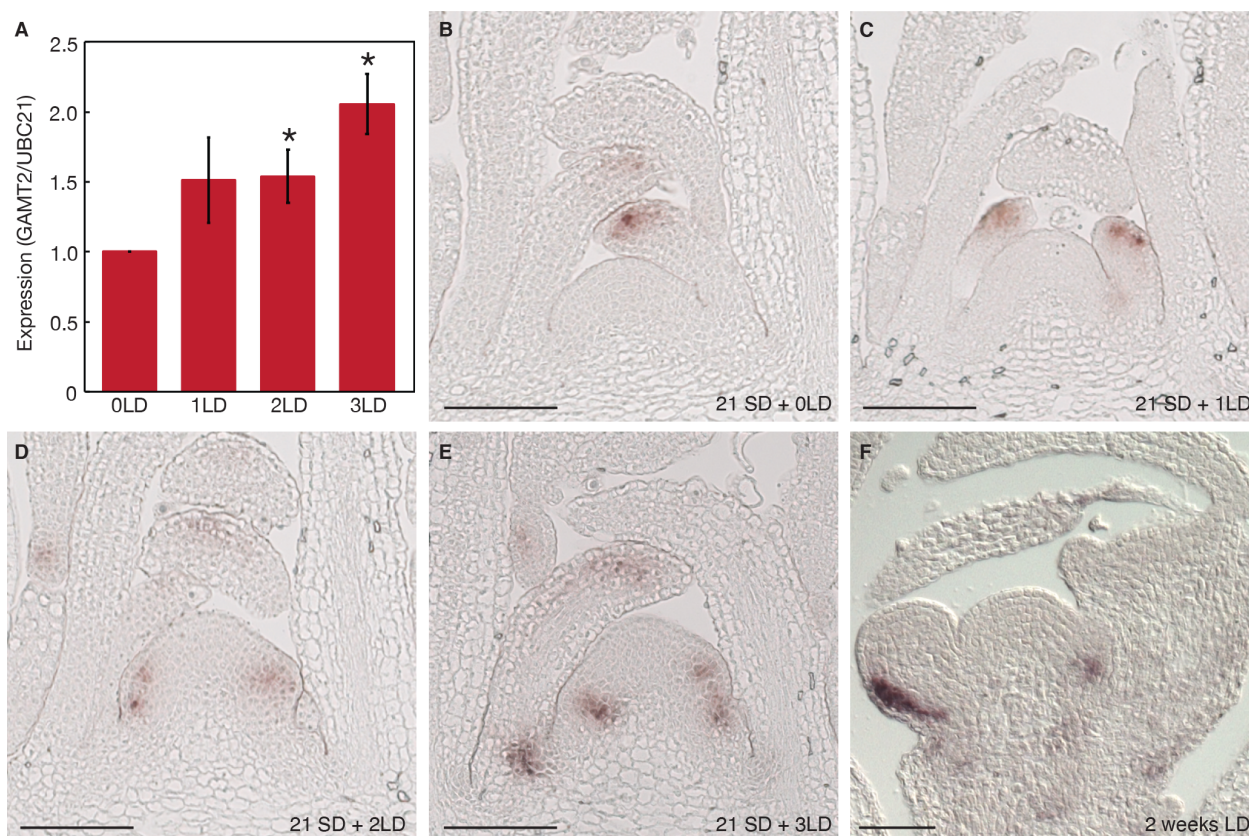


Fig. 1. *GAMT2* is induced at the shoot apical meristem during floral transition. (A) qPCR analysis of *GAMT2* expression in the shoot apices of Col-0 plants grown in SDs for 21 days then shifted to LDs for the indicated number of days. Values were normalised against the control gene *UBC21*, and columns show the mean of three biological replicates, \pm standard error. * $P < 0.05$ in Student's *t*-test. (B–E) RNA in situ hybridisation detection of *GAMT2* expression at the shoot apices of Col-0 plants grown in SDs for 21 days then shifted to LDs. (F) RNA in situ hybridisation detection of *GAMT2* expression in primary inflorescence of a Col-0 plant grown in LDs for 2 weeks. Scale bars = 50 μ m.

not be detected within the SAM (Fig. 1B,C). However, at 2 and 3 days after the shift to LDs, *GAMT2* expression was clearly observed at the flanks of the peripheral zone, specifically around the base of and overlapping with sites of incipient lateral organ primordia (Fig. 1D,E). The increase in *GAMT2* expression at the shoot apex that we detected by qPCR at the time of the floral commitment (Fig. 1A) therefore appears to be caused by an expansion of its expression domain within the SAM rather than an increase in expression level in the tips of leaf primordia. In later stages of flowering, strong *GAMT2* expression was also detected on the abaxial side of developing floral primordia but was not observed within the IM or in differentiated floral organs (Fig. 1F).

***gamt2* mutants are early flowering and display mild floral defects**

To investigate the potential role of *GAMT2* in floral transition, we obtained two T-DNA insertion mutants in the

Arabidopsis Col-0 background, the previously characterised null mutant *gamt2-1* (Varbanova et al. 2007), and *gamt2-3*, which has not previously been characterised (Fig. 2A). We confirmed that both are null alleles, with no expression of the exon 2 and exon 3 region of *GAMT2* detected by RT-PCR analysis (Fig. 2B), nor did we find any compensatory increase in the expression of *GAMT1* at the shoot apex in either of the *gamt2* mutant backgrounds (Fig. S2), indicating that *GAMT2* is the only one of the two GA methyltransferase enzymes that is likely to play a role in floral transition.

We found that the *gamt2-1* and *gamt2-3* mutants are both early flowering, as measured by total leaf number, when grown in LDs at either 22°C (day)/18°C (night) or constant 23°C (Fig. 2C,D; Appendix S1). This early flowering phenotype was mainly due to a decrease in the number of rosette leaves, whereas cauline leaf number was similar to or only slightly lower than that of wild-type plants. The consistent early flowering of two independent

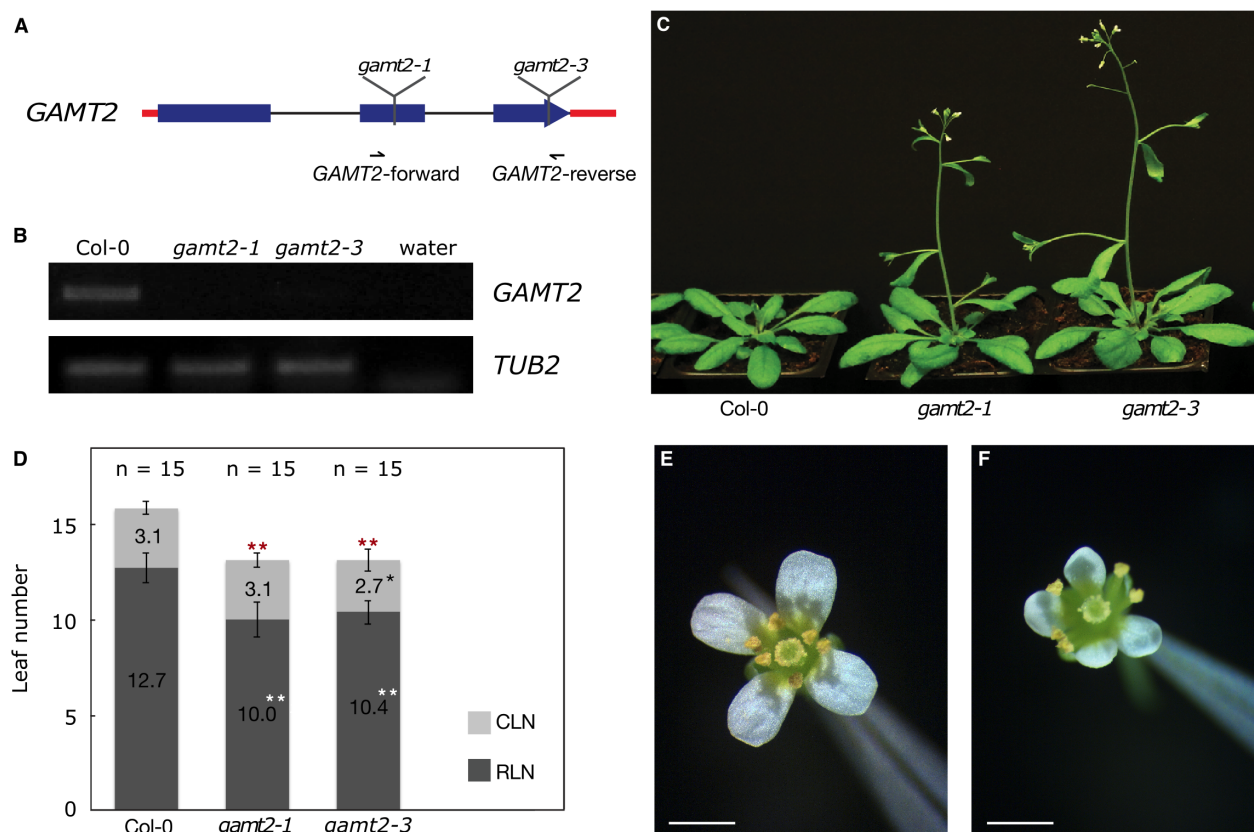


Fig. 2. Loss of *GAMT2* function accelerates flowering and affects floral patterning. (A) Gene model of *GAMT2*, showing the positions of the T-DNA insertions in *gamt2-1* and *gamt2-3* and the primers used for RT-PCR analysis. Red lines represent untranslated regions, black lines represent intron regions and blue boxes represent exons. (B) RT-PCR for *GAMT2* and *TUB2* transcripts in the siliques of Col-0, *gamt2-1* and *gamt2-3* plants. (C) Phenotypes of 25-day-old Col-0, *gamt2-1* and *gamt2-3* plants grown in 23°C LDs. (D) Flowering time of Col-0, *gamt2-1* and *gamt2-3* plants grown in 23°C LDs. Columns show the mean \pm standard error of cauline leaf number (CLN; light grey) and rosette leaf number (RLN; dark grey). Black, white and red stars indicate statistically significant differences in cauline, rosette and total leaf number, respectively, between *gamt2* mutants and wild-type plants. * $P < 0.05$; ** $P < 0.01$ in Student's *t*-test. (E) A normal Col-0 flower with six stamens. (F) A *gamt2-1* mutant flower with five stamens. Scale bars = 1 mm.

gamt2 mutants suggests that *GAMT2* plays a role in repressing flowering.

In addition to the early flowering phenotype, we also observed that the flowers of *gamt2* mutant plants often present mild patterning defects. In particular, 21.2% of *gamt2-1* flowers and 13.9% of *gamt2-3* flowers had only four or five stamens rather than the usual six, whereas this phenotype was observed in only 4.6% of examined flowers in wild-type plants (Fig. 2E,F; Table 1). This indicates that, in addition to a role in regulating floral transition, *GAMT2* also participates in organ patterning during flower formation.

***GAMT2* represses flowering at the SAM**

We next tested the effects of *GAMT2* misexpression. Previous studies have shown that ubiquitous *GAMT2* overexpression causes a suite of GA-deficient phenotypes

affecting whole-plant growth and development (Varbanova et al. 2007, Xing et al. 2007), which is consistent with *GAMT2*'s function as a GA-inactivating enzyme, but obscures the native role of *GAMT2* in any developmental processes involving more restricted spatiotemporal regulation. To mitigate this problem we therefore decided to generate a series of tissue-specific misexpression constructs in which *GAMT2* or an N-terminal VENUS-tagged version (VENUS-*GAMT2*) was placed under the control of a range of tissue-specific promoters that drive expression in regions around the shoot apex. The resulting transgenic lines are *pAt3g59270:GAMT2:tAt3g59270* and *pAt3g59270:VENUS-GAMT2:tAt3g59270* for misexpression in the entire SAM except for the outer two cell layers (L1 and L2) of the central zone (You et al. 2017) (Fig. 3A); *pLAS:VENUS-GAMT2:tLAS* for misexpression in boundary regions (Raatz et al. 2011) (Fig. 3B); and *pKNAT1:VENUS-GAMT2:tRBCS* for

Table 1 Frequency of floral defects in Col-0 and *gamt2* mutant plants.

Phenotype	Genotype		
	Col-0 (n = 109)	<i>gamt2-1</i> (n = 104)	<i>gamt2-3</i> (n = 108)
Six stamens (normal)	94.5%	75.0%	84.3%
Five stamens	3.6%	18.3%	13.0%
Four stamens	0.9%	2.9%	0.9%
Seven stamens	—	1.0%	—
Five sepals	—	1.0%	0.9%
Five sepals, five petals	—	1.0%	—
Fused stamens	—	—	0.9%
Petaloid stamen	0.9%	1.0%	—

misexpression mainly in the rib zone and in the vascular tissues underneath the SAM (Lincoln et al. 1994, An et al. 2004) (Fig. 3C). All the constructs were transformed into wild-type plants, and *VENUS-GAMT2* expression at the shoot apex was confirmed by fluorescence microscopy (Fig. S3).

Using these transgenic lines, we tested how misexpression of *GAMT2* in different domains of the SAM affects flowering time. When *VENUS-GAMT2* was misexpressed in the entire SAM except for L1 and L2 of the central zone, the transgenic T1 plants grew similarly to wild-type plants, without the visible GA-deficient phenotypes previously reported for *35S:GAMT2* plants (Varbanova et al. 2007, Xing et al. 2007), but they were significantly late-flowering, with approximately 6 more leaves on

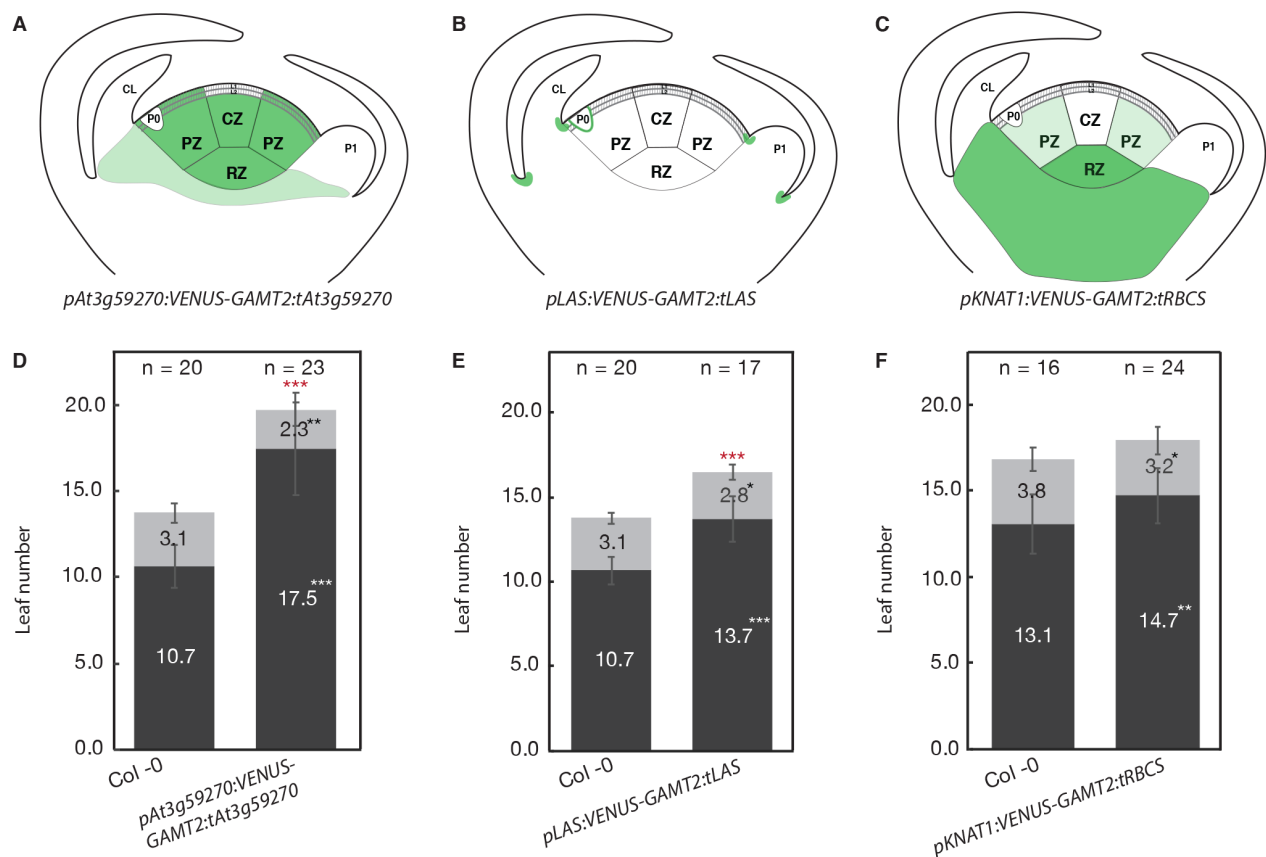


Fig. 3. Misexpression of *GAMT2* at the SAM delays flowering. (A–C) Schematic depictions of the expression domains of the *GAMT2* misexpression constructs (A) *pAt3g59270:VENUS-GAMT2:tAt3g59270*, (B) *pLAS:VENUS-GAMT2:tLAS* and (C) *pKNAT1:VENUS-GAMT2:tRBCS* in the transitioning SAM. Regions of *GAMT2* misexpression are shaded in green, with darker green representing areas of strong expression and lighter green representing weak expression. CZ, central zone, PZ, peripheral zone, RZ, rib zone, L1, layer 1, L2, layer 2, P0 and P1, floral primordia 0 and 1 and CL, cauline leaf. (D–F) Flowering time of (D) *pAt3g59270:VENUS-GAMT2:tAt3g59270*, (E) *pLAS:VENUS-GAMT2:tLAS* and (F) *pKNAT1:VENUS-GAMT2:tRBCS* T1 plants and Col-0 controls grown in 22°C/18°C LDs. Columns show the mean \pm standard error of cauline leaf number (light grey) and rosette leaf number (dark grey). Black, white and red stars indicate statistically significant differences in cauline, rosette and total leaf number, respectively, between transgenic and wild-type plants. * $P < 0.05$; ** $P < 0.01$; *** $P < 0.001$ in Student's *t*-test.

average than wild-type plants (Fig. 3D, Appendix S2). Interestingly, this difference was entirely due to an increase of approximately 6.8 rosette leaves, whereas cauline leaf number was reduced by approximately 0.8 in transgenic plants compared to wild-type. Similar though less pronounced phenotypes were observed when *VENUS-GAMT2* was misexpressed in boundary regions and in the rib meristem, with both the *pLAS:VENUS-GAMT2::tLAS* and *pKNAT1:VENUS-GAMT2* T1 populations producing significantly more rosette leaves but fewer cauline leaves than wild-type controls (Fig. 3E,F, Appendix S2). Similar late-flowering phenotypes were also observed in the T2 generations (Appendix S2). Overall, these results show that *GAMT2* delays the initial shift from VM to IM-I during floral transition when it is active in cells at the periphery of the SAM and organ boundaries, i.e. areas overlapping with the native expression domain of *GAMT2*. This is consistent with our prior observation that *gamt2* mutants are early flowering, and we therefore conclude that *GAMT2* is a repressor of flowering.

GAMT2* is not regulated by *LFY

Having established that *GAMT2* plays a role in the regulation of flowering time, we investigated why a repressor of flowering is induced specifically at the time of floral transition. We began by attempting to situate *GAMT2* within the network of known floral regulators, focusing on its relationship with the floral integrator *LFY*, as *GAMT2* was previously identified as a ‘high confidence’ *LFY* target gene in a chromatin immunoprecipitation coupled to microarray (ChIP-chip) experiment (Winter et al. 2011). Furthermore, *LFY* is expressed in leaf and floral primordia, the SAM periphery and floral meristems (Blazquez et al. 1997), in a pattern that partially overlaps with that of *GAMT2*, and *LFY* is known to be GA-regulated in SDs (Blazquez et al. 1998), as well as a regulator of GA levels in LDs (Yamaguchi et al. 2014). We therefore hypothesised that *LFY* might be a direct regulator of *GAMT2* expression.

To investigate this possibility, we retrieved the ChIP-chip data from Winter et al. (2011) and examined the two *LFY* binding peaks in the *GAMT2* promoter, and found that they each contained sequences corresponding to known *LFY* binding motifs. The first peak contained one primary and one secondary *LFY* binding motif (Winter et al. 2011), located approximately 3.7 and 3.6 kb upstream of the *GAMT2* transcription start site, respectively (sites 1 and 2), while the second peak contained a single primary motif located approximately 2.4 kb upstream of the *GAMT2* transcription start site (site 3) (Fig. 4A). We tested the physical interaction between

LFY and these putative *LFY* binding sites using yeast one-hybrid assays (Deplancke et al. 2006). Fragments of the *GAMT2* promoter containing the putative binding sites were placed upstream of a β -galactosidase reporter gene in DNA ‘bait’ constructs. We also generated a positive control containing a fragment of the *AP1* promoter that is known to be bound by *LFY* at the primary binding motif (Parcy et al. 1998). A separate ‘prey’ construct was generated in which the *LFY* coding sequence was placed downstream of the GAL4 activation domain (AD-*LFY*), and pairs of bait and prey constructs were transformed into yeast and tested for β -galactosidase activity (Fig. 4B). However, while a distinct blue colour reaction indicating reporter gene activation was observed for yeast carrying AD-*LFY* and the *AP1* promoter fragment, no colour reaction was detected for either of the two *GAMT2* promoter fragments, indicating that *LFY* does not activate these reporter constructs, at least in yeast cells.

We also assessed whether *LFY* might regulate *GAMT2* expression, either directly or indirectly, by examining the expression of *GAMT2* in a strong *lfy* mutant background, *lfy-12*. However, RNA in situ hybridisation showed that *GAMT2* is stably detected at shoot apices of *lfy-12* mutants (Fig. 4C,D) in a pattern similar to that observed in wild-type plants (Fig. 1B,E). We did observe a marked increase in *GAMT2* expression in *lfy-12* inflorescences compared to wild-type when measured by qPCR (Fig. 4E), but this may be due to *GAMT2* being expressed in the leaf-like ‘flowers’ produced by *lfy-12* mutants, rather than a release of *LFY*-mediated repression. Conversely, both RNA in situ hybridisation and qPCR analysis showed that *LFY* expression was unchanged in *gamt2-1* and *gamt2-3* mutants compared to wild-type plants, either before or after floral transition (Fig. 4F–H). Furthermore, the previous study by Winter et al. (2011) did not detect any significant change in *GAMT2* expression when *LFY* overexpression was induced. Overall, these data show no evidence of regulation in either direction between *GAMT2* and *LFY*, which suggests that, rather than acting in a common pathway, the two genes may perform parallel functions during floral transition.

***GAMT2* expression is induced by GA**

Negative feedback regulation has been shown to be important for GA homeostasis during plant growth and development, with GA levels often being fine-tuned through feedback loops between biosynthetic enzymes, inactivation enzymes and components of the GA signalling pathway (Zentella et al. 2007, Fukazawa et al. 2017), but it is not known if or how this type of feedback is involved in local developmental programs such as flowering time regulation (Eriksson et al. 2006). Given that

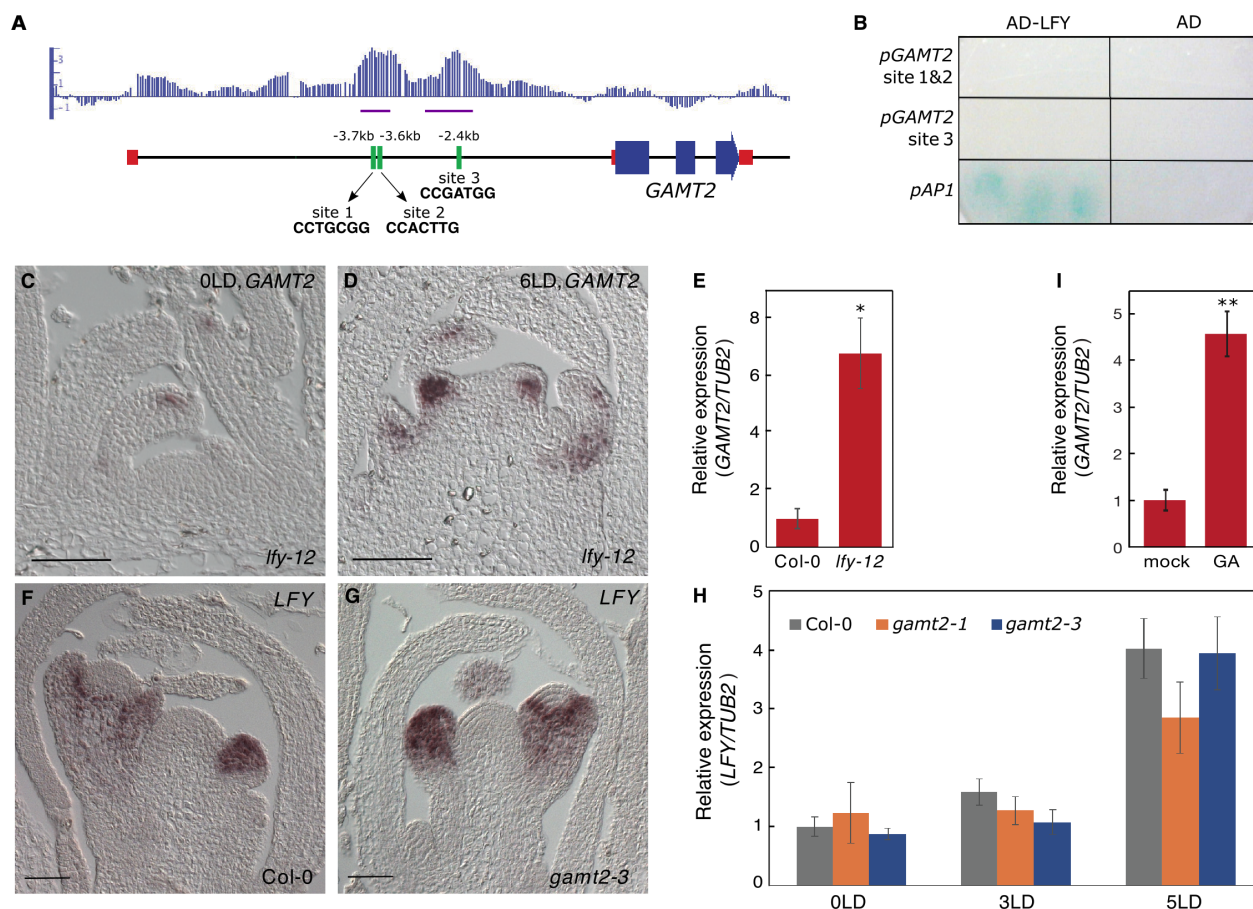


Fig. 4. *GAMT2* expression is not regulated by LFY but by GA. (A) Signal track of LFY binding at the *GAMT2* locus from published ChIP-chip data (Winter et al. 2011), with the positions and sequences of putative LFY binding motifs shown. The two *GAMT2* promoter fragments used in the yeast one-hybrid assays are shown as purple bars. (B) Yeast one-hybrid assays for binding of AD-LFY to the putative LFY binding sites from the *GAMT2* promoter. A fragment of the *AP1* promoter was used as a positive control and an empty AD construct was used as a negative control. Blue colour indicates β -galactosidase reporter activity arising from physical interaction between bait and prey constructs. (C and D) RNA in situ hybridisation detection of *GAMT2* expression in the shoot apices of *lfy-12* plants grown in SDs for (C) 21 days then shifted to LDs for (D) 6 days. (E) qPCR analysis of *GAMT2* expression in the primary inflorescences of LD-grown Col-0 and *lfy-12* plants. (F and G) RNA in situ hybridisation detection of *LFY* expression in the primary inflorescence of 14-day-old LD-grown (F) Col-0 and (G) *gamt2-3* plants. (H) qPCR analysis of *LFY* expression in the shoot apices of Col-0, *gamt2-1* and *gamt2-3* plants grown in SDs for 21 days and then shifted to LDs. (I) qPCR analysis of *GAMT2* expression in the shoot apices of 21-day-old SD-grown Col-0 plants 20 h after treatment with mock solution or exogenous GA₃. Scale bars in (C), (D), (F) and (G) = 50 μ m. For qPCR charts in (E), (H) and (I), values were normalised against the control gene *TUB2*, and columns show the mean of three biological replicates, \pm standard error. * $P < 0.05$; ** $P < 0.01$ in Student's *t*-test.

GA levels increase rapidly at the SAM during the transition to flowering, we hypothesised that *GAMT2* might be involved in a feedback loop to moderate or restrict this process.

To test our hypothesis, we examined the expression of *GAMT2* in the vegetative shoot apex of wild-type plants in response to treatments of either exogenous GA₃ or a mock solution. Our qPCR analysis showed that *GAMT2* expression was significantly increased by approximately 4.5-fold in the apices of GA₃-treated plants compared to controls at 20 h post-treatment (Fig. 4I). This is

consistent with a previous study which found that *GAMT2* expression was upregulated in plants that had increased levels of endogenous GAs arising from over-expression of the GA biosynthetic gene *GA20ox1* (Nam et al. 2017). Taken together, our results suggest that *GAMT2* expression is induced in response to an initial increase in GA levels at the SAM during the early stages of floral transition, and that the enzyme acts in a local negative feedback loop to regulate the amount of GA in the peripheral and boundary regions of the shoot apex.

Discussion

Spatiotemporal regulation of GA at the SAM contributes to the timing of flowering in LDs

Genetic analyses in *Arabidopsis* have identified a number of molecular pathways that perceive and integrate diverse endogenous and environmental signals to ensure that flowering occurs under the conditions most favourable for reproductive success (Srikanth and Schmid 2011). The GA pathway is essential for flowering under SD conditions, with bioactive GAs gradually increasing at the SAM and promoting the expression of floral integrators *SOC1* and *LFY*, whereas the photoperiodic pathway is the key driver of floral transition under LDs, acting through *CONSTANS* (CO) and its transcriptional targets, the floral activators *FT* and *TSF* (Fornara et al. 2010, Srikanth and Schmid 2011). However, GA is still highly important for flowering in LDs, as GA promotes the expression of *FT* and *TSF* in leaves independently of CO (Galvao et al. 2012), and genetic approaches that reduce GA levels or inhibit GA signalling can severely delay flowering in LDs (Griffiths et al. 2006, Hu et al. 2008, Galvao et al. 2012, Porri et al. 2012, Richter et al. 2013).

While it is clear that GAs play an important role in the regulation of flowering time in LDs, this process appears to involve complex spatiotemporal regulation and is not well understood. A previous study showed that, under inductive LDs, the GA biosynthetic gene *GA20ox2* is strongly expressed in the rib zone, and the resulting rise in bioactive GA levels is suggested to promote flowering and stem elongation (Andres et al. 2014). Interestingly, it has also been shown that the GA-inactivating *ELA1* gene is expressed on the abaxial side of incipient flower primordia during LD-induced flowering, and that mutations in *ELA1* have no effect on rosette leaf number, but significantly increase cauline leaf number (Yamaguchi et al. 2014). It was therefore suggested that GA plays two opposing roles in flowering, promoting the transition from vegetative to reproductive growth but inhibiting the acquisition of floral identity in lateral organ primordia produced by the IM (Yamaguchi et al. 2014). In this study, we show that, in addition to triggering an increase in GA biosynthesis, LDs also induce expression of *GAMT2* in the peripheral zone of the SAM, which might trigger a negative feedback loop restricting the rise in bioactive GA levels during floral transition. This mechanism may help plants to moderate and/or restrict the spatial distribution of the high levels of bioactive GA₄ synthesised by GA20ox in the rib meristem. Furthermore, when we examined RNA-seq data from a recent study investigating the genome-wide targets of FD (Collani et al. 2019), we found that LD-induced *GAMT2* expression appears to

be dependent on FD activity (Fig. S4). This effect is likely indirect, as *GAMT2* was not among the direct targets of FD, but it is interesting to note that FD has recently been shown to play a central role in regulating the crosstalk between flowering pathways and hormone signalling pathways at the SAM (Collani et al. 2019). It may be useful for future research to examine this regulatory relationship more closely, to better understand the interaction between GA metabolism and the photoperiodic pathway in the control of flowering time at the SAM.

GA inactivation enzymes support SAM function and development

GA levels are controlled through both biosynthesis and inactivation pathways. The major pathway for inactivating bioactive GAs is through GA 2-oxidation, and a number of GA2ox enzymes have been identified in various plant species (Rieu et al. 2008). Two other mechanisms of GA inactivation have also been reported in a more limited number of species: epoxidation by the cytochrome P450 monooxygenases *ELA1* and *ELA2* in *Arabidopsis* and their homologue *ELONGATED UPPERMOST INTERNODE1* (*EUI1*) in rice (Nomura et al. 2013), and methylation by the GA methyltransferases *GAMT1* and *GAMT2*, which have so far only been described in *Arabidopsis* (Varbanova et al. 2007, Xing et al. 2007).

Previous studies indicate that GAs are kept at low levels in the vegetative SAM through the activity of the KNOX family transcription factors, in order to prevent differentiation and maintain meristem identity, while in the initiating lateral organ primordia, GA level rises and promotes cell differentiation and organ development (Veit 2009, Hay and Tsiantis 2010). This model is not derived from direct measurement of GA levels, which is technically challenging in such small tissues, but is based instead on experiments showing that KNOX proteins in the SAM directly inhibit the GA biosynthetic gene *GA20ox1* and activate the GA inactivation gene *GA2ox1*, in *Arabidopsis* as well as in maize and tobacco (Sakamoto et al. 2001, Jasinski et al. 2005, Yanai et al. 2005, Bolduc and Hake 2009). Reporter gene assays and RNA in situ hybridisation show that the genes encoding GA2ox enzymes are not expressed throughout the entire KNOX expression domain, but are mainly active below the SAM and at the base of developing leaf primordia, and it has been suggested that this sets boundaries to prevent diffusion of bioactive GAs from lateral organs or the stem into the SAM, thereby preserving meristem function (Sakamoto et al. 2001, Jasinski et al. 2005, Yanai et al. 2005, Bolduc and Hake 2009, Veit 2009, Hay and Tsiantis 2010).

It is interesting to note that the expression pattern of the *GA2ox* genes bears some similarity to that of *GAMT2*, although *GAMT2* is limited to the tips of leaf primordia during vegetative growth and only appears at the periphery and boundaries of the SAM during floral transition. It remains to be seen whether *GAMT2* expression is also controlled by KNOX transcription factors or has any involvement in the maintenance of meristematic pluripotency. Notwithstanding the similar spatial expression patterns of *GAMT2* and the *GA2ox* genes, the two types of enzymes do not appear to be redundant with each other, since they are active at different stages of development and *GA2ox* genes have dynamic and diverse changes in expression during floral transition (Fig. S5). *GAMT2* appears to have a specialised role in floral transition, possibly because increases in GA levels, SAM plasticity and cell proliferation during flowering create an increased requirement for strict regulation of tissue boundaries. *GAMT2* may contribute to this regulation simply as an additional layer of control, or it may have a functionally different role to that of the *GA2ox* enzymes. The products of GA 2-oxidation accumulate in planta and can readily be detected even in *ga2ox* quintuple mutants (Rieu et al. 2008), whereas the products of GA methylation are not detected either in wild-type *Arabidopsis* or in plants overexpressing *GAMT1* or *GAMT2* (Varbanova et al. 2007). It is not known what happens to the methylated GAs, but it has been suggested that methylation is the first step in an irreversible process of deactivation and degradation, which would account for their failure to accumulate to detectable levels in planta (Varbanova et al. 2007). Inactivation of GAs through methylation rather than 2-oxidation may therefore enable the rapid depletion of excess GAs to prevent premature flowering in response to stochastic or transient increases in GA, and/or to more efficiently maintain tissue boundaries and meristem function.

Influence of GA on flower formation

In SDs, GA promotes expression of the floral meristem identity gene *LFY* to trigger floral commitment, but the details of GA regulation of flowering in LDs are less well characterised. However, it has been shown that *LFY* and *AP1* directly promote *ELA1* expression in LDs, and the decrease in bioactive GA levels caused by *ELA1* activity is required for the inflorescence meristem to switch from cauline leaf to flower formation (Yamaguchi et al. 2014, Winter et al. 2015). RNA in situ hybridisation and reporter gene assays shows that *ELA1* is initially expressed on the abaxial side of young floral primordia, and later along their entire circumference, but it is never

detected in either the VM or the IM (Yamaguchi et al. 2014, Winter et al. 2015). In our study, we showed that *GAMT2* was strongly expressed in the peripheral zone of the SAM during floral transition (Fig. 1D,E), but after the switch to flower formation, it disappeared from the IM and could only be detected on the abaxial side of floral primordia (Fig. 1F). As to the effects on flowering time, loss of *GAMT2* function results in early flowering, with a decrease in both rosette and cauline leaf numbers, whereas loss of *ELA1* function does not affect rosette leaf number but significantly increases cauline leaf number. Furthermore, *ELA1* is a direct target of both *LFY* and *AP1*, whereas our data demonstrated that *GAMT2* expression is very likely not regulated by *LFY*, and *gamt2* mutations had no effect on *LFY* or *AP1* expression (Figs 4C-H and S6). Therefore, despite the two genes encoding enzymes with similar functions and having overlapping spatiotemporal expression patterns in floral primordia, they do not seem to be functionally redundant in the regulation of flowering.

The fact that misexpression of *GAMT2* at the shoot apex typically causes increased rosette leaf number but decreased cauline leaf number (Fig. 3D-F, Appendix S2) is consistent with what is currently known about GA's opposing roles in promoting the initial transition to flowering but repressing flower formation (Yamaguchi et al. 2014), but it is intriguing that *gamt2* mutants also have similar or slightly lower numbers of cauline leaves compared to wild-type plants, in addition to significantly decreased numbers of rosette leaves (Fig. 2D, Appendix S1). A possible explanation for this is that *GAMT2* normally acts primarily as a repressor of the VM to IM-I transition, such that loss of *GAMT2* activity in *gamt2* mutants accelerates floral transition without directly affecting the timing of flower formation, whereas in the transgenic plants, excessively high levels of misexpressed *GAMT2* may cause a severe decrease in bioactive GA levels at the SAM throughout both stages of inflorescence development, so that it represses the VM to IM-I transition more strongly than it does when present at wild-type levels, and also accelerates the IM-I to IM-II transition in the same manner that *ELA1* normally does. Taken together, these results indicate that *GAMT2*-mediated inactivation of GA in the peripheral zone of the SAM is important for regulating the initial floral transition, while *ELA1*-mediated inactivation controls the subsequent transition from cauline leaf to flower formation. Further research will be needed to clarify the precise mechanisms involved and to investigate if and how these enzymes differ from each other functionally, and why they are each used for such distinct roles.

Author contributions

J.E.L., Y.Y. and M.S. designed the experiments; J.E.L. and Y.Y. performed most of the experiments; D.G. participated in the work of microscopy and flowering-time phenotyping; M.N. participated in the work of cloning and qPCR; J.E.L., Y.Y. and M.S. analysed the results and wrote the manuscript, with input from other co-authors.

Acknowledgements – We thank Professor Detlef Weigel from the Max Planck Institute for Developmental Biology for contributing the seeds of *lfy-12* and *ap1-15* mutants; Professor Alexis Maizel from the University of Heidelberg for contributing the pAM190 plasmid; and Andrew Balmer and Joachim Forner from the University of Heidelberg for contributing some of the GreenGate cloning modules. We thank Silvio Collani from Umeå University for providing RNA-seq data; and Natalie Agarwala and Damaris Kust, student helpers from the University of Tübingen, for technical assistance. This work was supported by infrastructure grants from VINNOVA (2016-00504) and the Knut and Alice Wallenberg Foundation (2016.0341) to the Umeå Plant Science Centre; a post-doctoral fellowship from the Max Planck Society to Y.Y.; the Institutional Strategy Program of the University of Tübingen (DFG, ZUK 63) and the DFG (No. 427105396) to Y.Y.; grants from the DFG for the ERA-CAPS project 'FlowPlast' to M.S. (SCHM 1560/10–1); and the Knut and Alice Wallenberg Foundation to M.S. (2016.0025).

Data availability statement

The data that support the findings of this study are available upon reasonable request. Persons responsible for distribution of material are the corresponding authors Y. Y. (yuan.you@zmbp.uni-tuebingen.de) and M.S. (markus.schmid@umu.se).

References

- An H, Roussot C, Suárez-López P, Corbesier L, Vincent C, Piñeiro M, Hepworth S, Mouradov A, Justin S, Turnbull C, Coupland G (2004) CONSTANS acts in the phloem to regulate a systemic signal that induces photoperiodic flowering of *Arabidopsis*. *Development* 131: 3615–3626
- Andres F, Porri A, Torti S, Mateos J, Romera-Branchat M, Garcia-Martinez JL, Fornara F, Gregis V, Kater MM, Coupland G (2014) SHORT VEGETATIVE PHASE reduces gibberellin biosynthesis at the *Arabidopsis* shoot apex to regulate the floral transition. *Proc Natl Acad Sci USA* 111: 2760–2769
- Bao S, Hua C, Shen L, Yu H (2020) New insights into gibberellin signaling in regulating flowering in *Arabidopsis*. *J Integr Plant Biol* 62: 118–131
- Blazquez MA, Weigel D (2000) Integration of floral inductive signals in *Arabidopsis*. *Nature* 404: 889–892
- Blazquez MA, Soowal LN, Lee I, Weigel D (1997) LEAFY expression and flower initiation in *Arabidopsis*. *Development* 124: 3835–3844
- Blazquez MA, Green R, Nilsson O, Sussman MR, Weigel D (1998) Gibberellins promote flowering of *Arabidopsis* by activating the LEAFY promoter. *Plant Cell* 10: 791–800
- Bolduc N, Hake S (2009) The maize transcription factor KNOTTED1 directly regulates the gibberellin catabolism gene *ga2ox1*. *Plant Cell* 21: 1647–1658
- Clough SJ, Bent AF (1998) Floral dip: a simplified method for agrobacterium-mediated transformation of *Arabidopsis thaliana*. *Plant J* 16: 735–743
- Collani S, Neumann M, Yant L, Schmid M (2019) FT modulates genome-wide DNA-binding of the bZIP transcription factor FD. *Plant Physiol* 180: 367–380
- Deplancke B, Vermeirssen V., Arda H.E., Martinez N.J., Walhout A.J.M. (2006) Gateway-Compatible Yeast One-Hybrid Screens. *Cold Spring Harbor Protocols*, 2006 (28), pdb.prot4590–pdb.prot4590. <http://dx.doi.org/10.1101/pdb.prot4590>.
- Eriksson S, Bohlenius H, Moritz T, Nilsson O (2006) GA4 is the active gibberellin in the regulation of LEAFY transcription and *Arabidopsis* floral initiation. *Plant Cell* 18: 2172–2181
- Fornara F, de Montaigu A, Coupland G (2010) SnapShot: control of flowering in *Arabidopsis*. *Cell* 141 550: e1–e2
- Fukazawa J, Mori M, Watanabe S, Miyamoto C, Ito T, Takahashi Y (2017) DELLA-GAF1 complex is a main component in gibberellin feedback regulation of GA20 oxidase 2. *Plant Physiol* 175: 1395–1406
- Galvao VC, Horrer D, Kuttner F, Schmid M (2012) Spatial control of flowering by DELLA proteins in *Arabidopsis thaliana*. *Development* 139: 4072–4082
- Gocal GF, King RW, Blundell CA, Schwartz OM, Andersen CH, Weigel D (2001) Evolution of floral meristem identity genes. Analysis of *Lolium temulentum* genes related to APETALA1 and LEAFY of *Arabidopsis*. *Plant Physiol* 125: 1788–1801
- Griffiths J, Murase K, Rieu I, Zentella R, Zhang ZL, Powers SJ, Gong F, Phillips AL, Hedden P, Sun TP, Thomas SG (2006) Genetic characterization and functional analysis of the GID1 gibberellin receptors in *Arabidopsis*. *Plant Cell* 18: 3399–3414
- Hay A, Tsiantis M (2010) KNOX genes: versatile regulators of plant development and diversity. *Development* 137: 3153–3165
- Hay A, Kaur H, Phillips A, Hedden P, Hake S, Tsiantis M (2002) The gibberellin pathway mediates KNOTTED1-type homeobox function in plants with different body plans. *Curr Biol* 12: 1557–1565
- Hu J, Mitchum MG, Barnaby N, Ayele BT, Ogawa M, Nam E, Lai WC, Hanada A, Alonso LM, Ecker LR, Swain SM, Yamaguchi S, Kamiya Y, Sun TP (2008) Potential sites of bioactive gibberellin production during reproductive growth in *Arabidopsis*. *Plant Cell* 20: 320–336

- Immink RGH, Pose D, Ferrario S, Ott F, Kaufmann K, Valentim FL, de Folter S, van der Wal F, van Dijk ADJ, Schmid M, Angenent GC (2012) Characterization of SOC1's central role in flowering by the identification of its upstream and downstream regulators. *Plant Physiol* 160: 433–449
- Jasinski S, Piazza P, Craft J, Hay A, Woolley L, Rieu I, Phillips A, Hedden P, Tsiantis M (2005) KNOX action in Arabidopsis is mediated by coordinate regulation of cytokinin and gibberellin activities. *Curr Biol* 15: 1560–1565
- Lampropoulos A, Sutikovic Z, Wenzl C, Maegele I, Lohmann JU, Forner J (2013) GreenGate – a novel, versatile, and efficient cloning system for plant transgenesis. *PLoS One* 8: e83043
- Lincoln C, Long J, Yamaguchi J, Serikawa K, Hake S (1994) A knotted1-like homeobox gene in Arabidopsis is expressed in the vegetative meristem and dramatically alters leaf morphology when overexpressed in transgenic plants. *Plant Cell* 6: 1859–1876
- Moon J, Suh SS, Lee H, Choi KR, Hong CB, Paek NC, Kim SG, Lee I (2003) The SOC1 MADS-box gene integrates vernalization and gibberellin signals for flowering in Arabidopsis. *Plant J* 35: 613–623
- Nam YJ, Herman D, Blomme J, Chae E, Kojima M, Coppens F, Storme V, Van Daele T, Dhondt S, Sakakibara H, Weigel D, Inze D, Gonzalez N (2017) Natural variation of molecular and morphological gibberellin responses. *Plant Physiol* 173: 703–714
- Ng M, Yanofsky MF (2001) Activation of the Arabidopsis B class homeotic genes by APETALA1. *Plant Cell* 13: 739–753
- Nomura T, Magome H, Hanada A, Takeda-Kamiya N, Mander LN, Kamiya Y, Yamaguchi S (2013) Functional analysis of Arabidopsis CYP714A1 and CYP714A2 reveals that they are distinct gibberellin modification enzymes. *Plant Cell Physiol* 54: 1837–1851
- Olszewski N, Sun TP, Gubler F (2002) Gibberellin signaling: biosynthesis, catabolism, and response pathways. *Plant Cell* 14: S61–S80
- Parcy F, Nilsson O, Busch MA, Lee I, Weigel D (1998) A genetic framework for floral patterning. *Nature* 395: 561–566
- Porri A, Torti S, Romera-Branchat M, Coupland G (2012) Spatially distinct regulatory roles for gibberellins in the promotion of flowering of Arabidopsis under long photoperiods. *Development* 139: 2198–2209
- Ratz B, Eicker A, Schmitz G, Fuss E, Muller D, Rossmann S, Theres K (2011) Specific expression of LATERAL SUPPRESSOR is controlled by an evolutionarily conserved 3' enhancer. *Plant J* 68: 400–412
- Ratcliffe OJ, Bradley DJ, Coen ES (1999) Separation of shoot and floral identity in Arabidopsis. *Development* 126: 1109–1120
- Richter R, Bastakis E, Schwechheimer C (2013) Cross-repressive interactions between SOC1 and the GATAs GNC and GNL/CGA1 in the control of greening, cold tolerance, and flowering time in Arabidopsis. *Plant Physiol* 162: 1992–2004
- Rieu I, Eriksson S, Powers SJ, Gong F, Griffiths J, Woolley L, Benlloch R, Nilsson O, Thomas SG, Hedden P, Phillips AL (2008) Genetic analysis reveals that C19-GA 2-oxidation is a major gibberellin inactivation pathway in Arabidopsis. *Plant Cell* 20: 2420–2436
- Sakamoto T, Kamiya N, Ueguchi-Tanaka M, Iwahori S, Matsuoka M (2001) KNOX homeodomain protein directly suppresses the expression of a gibberellin biosynthetic gene in the tobacco shoot apical meristem. *Genes Dev* 15: 581–590
- Schmid M, Davison TS, Henz SR, Pape UJ, Demar M, Vingron M, Scholkopf B, Weigel D, Lohmann JU (2005) A gene expression map of *Arabidopsis thaliana* development. *Nat Genet* 37: 501–506
- Scofield S, Murison A, Jones A, Fozard J, Aida M, Band LR, Bennett M, Murray JAH (2018) Coordination of meristem and boundary functions by transcription factors in the SHOOT MERISTEMLESS regulatory network. *Development* 145: dev157081
- Srikanth A, Schmid M (2011) Regulation of flowering time: all roads lead to Rome. *Cell Mol Life Sci* 68: 2013–2037
- Varbanova M, Yamaguchi S, Yang Y, McKelvey K, Hanada A, Borochoy R, Yu F, Jikumaru Y, Ross J, Cortes D, Ma CJ, Noel JP, Mander L, Shulaev V, Kamiya Y, Rodermel S, Weiss D, Pichersky E (2007) Methylation of gibberellins by Arabidopsis GAMT1 and GAMT2. *Plant Cell* 19: 32–45
- Veit B (2009) Hormone mediated regulation of the shoot apical meristem. *Plant Mol Biol* 69: 397–408
- Wang JW, Czech B, Weigel D (2009) miR156-regulated SPL transcription factors define an endogenous flowering pathway in *Arabidopsis thaliana*. *Cell* 138: 738–749
- Weigel D, Jurgens G (2002) Stem cells that make stems. *Nature* 415: 751–754
- Wilczek AM, Roe JL, Knapp MC, Cooper MD, Lopez-Gallego C, Martin LJ, Muir CD, Sim S, Walker A, Anderson J, Egan JF, Moyers BT, Petipas R, Giakountis A, Charbit E, Coupland G, Welch SM, Schmitt J (2009) Effects of genetic perturbation on seasonal life history plasticity. *Science* 323: 930–934
- Winter CM, Austin RS, Blanvillain-Baufume S, Reback MA, Monniaux M, Wu MF, Sang Y, Yamaguchi A, Yamaguchi N, Parker JE, Parcy F, Jensen ST, Li H, Wagner D (2011) LEAFY target genes reveal floral regulatory logic, cis motifs, and a link to biotic stimulus response. *Dev Cell* 20: 430–443
- Winter CM, Yamaguchi N, Wu MF, Wagner D (2015) Transcriptional programs regulated by both LEAFY and APETALA1 at the time of flower formation. *Physiol Plant* 155: 55–73
- Xing SF, Qin GJ, Shi Y, Ma ZQ, Chen ZL, Gu HY, Qu LJ (2007) GAMT2 encodes a methyltransferase of gibberellin

acid that is involved in seed maturation and germination in Arabidopsis. *J Integr Plant Biol* 49: 368–381

Yamaguchi N, Winter CM, Wu MF, Kanno Y, Yamaguchi A, Seo M, Wagner D (2014) Gibberellin acts positively then negatively to control onset of flower formation in Arabidopsis. *Science* 344: 638–641

Yanai O, Shani E, Dolezal K, Tarkowski P, Sablowski R, Sandberg G, Samach A, Ori N (2005) Arabidopsis KNOX proteins activate cytokinin biosynthesis. *Curr Biol* 15: 1566–1571

You Y, Sawikowska A, Neumann M, Pose D, Capovilla G, Langenecker T, Neher RA, Krajewski P, Schmid M (2017) Temporal dynamics of gene expression and histone marks at the Arabidopsis shoot meristem during flowering. *Nat Commun* 8: 15120

You Y, Sawikowska A, Lee JE, Benstein RM, Neumann M, Krajewski P, Schmid M (2019) Phloem companion cell-specific transcriptomic and epigenomic analyses identify MRF1, a regulator of flowering. *Plant Cell* 31: 325–345

Zentella R, Zhang ZL, Park M, Thomas SG, Endo A, Murase K, Fleet CM, Jikumaru Y, Nambara E, Kamiya Y, Sun TP (2007) Global analysis of della direct targets in early gibberellin signaling in Arabidopsis. *Plant Cell* 19: 3037–3057

Supporting information

Additional supporting information may be found online in the Supporting Information section at the end of the article.

Fig. S1. Tissue-specific expression of *ELA1*, *LFY*, *GAMT1* and *GAMT2* throughout development.

Fig. S2. qPCR analysis of *GAMT1* expression in the shoot apices of 14-day-old LD-grown Col-0, *gamt2-1* and *gamt2-3* plants.

Fig. S3. Fluorescence microscopy of *GAMT2* misexpression constructs.

Fig. S4. Expression of *GAMT2* in the shoot apices of phenotypically wild-type *pFD:GFP-FD fd-2* and *fd-2* mutant plants.

Fig. S5. Expression of *GAMT2* and *GA2ox* family genes in vegetative, transition and inflorescence shoot apices during floral transition.

Fig. S6. qPCR analysis of *GAMT2* and *AP1* expression.

Table S1. Sequences of oligonucleotide primers used in this work.

Table S2. GreenGate cloning modules.

Appendix S1. Flowering time of wild-type Col-0, *gamt2-1* and *gamt2-3* plants.

Appendix S2. Flowering time of *GAMT2* misexpression lines.